

Simulation of light intensity dependent current characteristics of polymer solar cells

Pavel Schilinsky, Christoph Waldauf, Jens Hauch, and Christoph J. Brabec

Citation: *J. Appl. Phys.* **95**, 2816 (2004); doi: 10.1063/1.1646435

View online: <http://dx.doi.org/10.1063/1.1646435>

View Table of Contents: <http://jap.aip.org/resource/1/JAPIAU/v95/i5>

Published by the [American Institute of Physics](#).

Related Articles

Correlation between interface energetics and open circuit voltage in organic photovoltaic cells
[Appl. Phys. Lett. 101, 233301 \(2012\)](#)

Correlation between interface energetics and open circuit voltage in organic photovoltaic cells
[APL: Org. Electron. Photonics 5, 259 \(2012\)](#)

New method to assess the loss parameters of the photovoltaic modules
[J. Renewable Sustainable Energy 4, 063115 \(2012\)](#)

Electric double layers allow for opaque electrodes in high performance organic optoelectronic devices
[APL: Org. Electron. Photonics 5, 236 \(2012\)](#)

Electric double layers allow for opaque electrodes in high performance organic optoelectronic devices
[Appl. Phys. Lett. 101, 173302 \(2012\)](#)

Additional information on J. Appl. Phys.

Journal Homepage: <http://jap.aip.org/>

Journal Information: http://jap.aip.org/about/about_the_journal

Top downloads: http://jap.aip.org/features/most_downloaded

Information for Authors: <http://jap.aip.org/authors>

ADVERTISEMENT

The advertisement banner for AIP Advances features a green and yellow background with abstract wavy lines. The AIP Advances logo is prominently displayed in the center, with the word 'AIP' in blue and 'Advances' in green. To the right, a circular badge states 'Now Indexed in Thomson Reuters Databases'. Below the logo, the text 'Explore AIP's open access journal:' is followed by a list of three bullet points: 'Rapid publication', 'Article-level metrics', and 'Post-publication rating and commenting'.

AIPAdvances

Now Indexed in Thomson Reuters Databases

Explore AIP's open access journal:

- Rapid publication
- Article-level metrics
- Post-publication rating and commenting

Simulation of light intensity dependent current characteristics of polymer solar cells

Pavel Schilinsky^{a)} and Christoph Waldauf

Energy and Semiconductor Research Laboratory, Faculty of Physics, University of Oldenburg, D-26111 Oldenburg, Germany and SIEMENS AG, CT MM1, Innovative Polymers, Paul Gossenstr. 100, D-91052 Erlangen, Germany

Jens Hauch and Christoph J. Brabec

SIEMENS AG, CT MM1, Innovative Polymers, Paul Gossenstr. 100, D-91052 Erlangen, Germany

(Received 5 June 2003; accepted 16 December 2003)

An extended replacement circuit describing the current–voltage characteristics of bulk heterojunction polymer solar cells at different light bias levels is introduced and discussed. A one diode-model is expanded by an extraction model for photogenerated carriers taking into account the effective reduction of the mean distance which the charge carriers cover when sweeping the electrical bias through the fourth quadrant of the solar cell. The model properly describes the current–voltage behavior of bulk heterojunction solar cells over more than three orders in light intensity with one set of parameters. © 2004 American Institute of Physics.
[DOI: 10.1063/1.1646435]

INTRODUCTION

Polymeric bulk heterojunction solar cells and photodetectors have attracted a lot of attention¹ due to their high potential in cost reduction for large area elements. In contrast to classical bilayer junction devices, a bulk heterojunction device consists of a more or less homogenous mixture of donor and acceptor materials, where at most times the donor is a conjugated polymer and the acceptor a fullerene.² The active layer of a bulk heterojunction is typically embedded between two electrodes, similar to metal–insulator–metal or Schottky type devices. Recent progress shows power conversion efficiencies of 3.5%³ and external quantum efficiencies as high as 76% at 560 nm.⁴ While short circuit current densities of over 10 mA/cm² under one sun are promising values for organic photovoltaic devices, both, the fill factor (FF) and the open circuit voltage (V_{oc}) are disappointingly low. While the optical band gap of the active layer is typically ~ 2 eV, the open circuit voltage of bulk heterojunction device is only between 500 and 800 mV, depending on the position of the highest occupied molecular orbit (HOMO) of the donor polymer. While this behavior can be understood from HOMO/lowest unoccupied molecular orbit (LUMO) models,⁵ no simple models are available which describe the device performance by taking into account the light intensity. However, in order to further optimize these devices, and explain the dependence of the FF and V_{oc} with the light intensity, models are needed to describe the light dependent processes in bulk heterojunction solar cells. In this article an extension of the standard one diode model is introduced, which allows the simulation of I – V curves measured under different light intensities.

MODEL PRINCIPLES AND RESULTS

In a recent publication we have described the current–voltage characteristics of bulk heterojunction solar cells by solving the transport equations self-consistently with the electrical field. These simulations showed that a bulk heterojunction composite can be successfully described by a single intrinsic semiconductor layer with the energy levels of the valence and conduction band as the HOMO of the polymer and the LUMO of the fullerene, respectively.³

Based on the self-consistent solutions to the transport equations the electrical field in the active layer of the bulk heterojunction solar cells is calculated. The electrical field is found to be constant over the active layer and no or negligible deviation from this behavior is observed under intense illumination (Fig. 1). Based on this finding, a macroscopic replacement circuit is suggested, capable of describing the current–voltage characteristics of bulk heterojunction solar cells under different illumination densities with a single set of parameters. Such a replacement circuit has to take the field dependence of the photocurrent into account.

Before describing the expanded replacement circuit, the deficiencies of the standard one diode model⁶ are discussed when applied to describe the current–voltage characteristics of bulk heterojunction solar cells. The model is given by Eq. (1) and schematically depicted in Fig. 2. Here, the photoinduced current I_{light} is added as a current source

$$I - I_0 \times \left[e^{e \times (V - I \times R_s) / nk_B T} - 1 \right] - \frac{V - I \times R_s}{R_p} + I_{light} = 0, \quad (1)$$

where I is the current through the diode, I_0 is the saturation current, k_B is the Boltzmann constant, T is the temperature in Kelvin, V is the external bias applied to the diode, n is the ideality factor of the diode, R_s is the serial resistance, and R_p is the parallel resistance. The dependence of the parallel re-

^{a)}Electronic mail: schilinsky@ivopavel.de

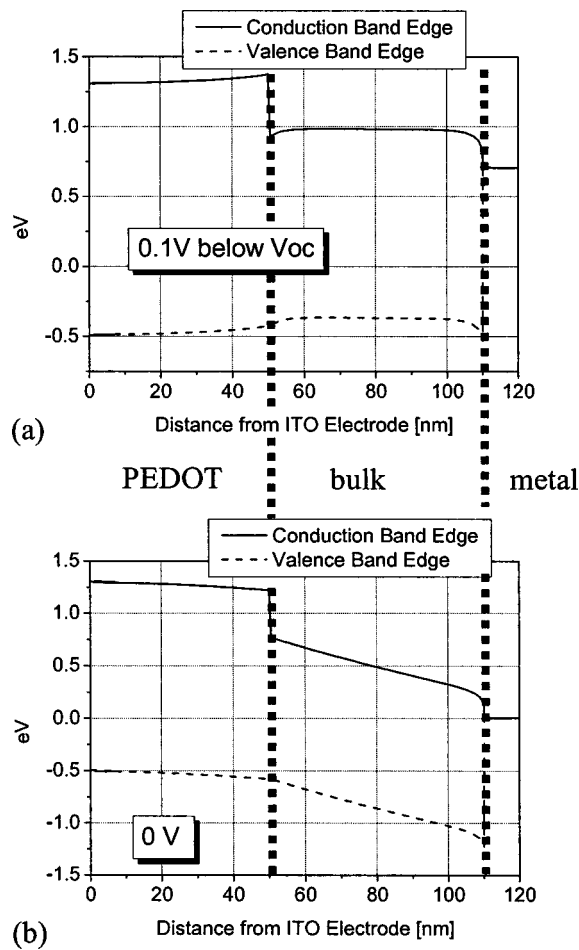


FIG. 1. Dependence of the electrical potentials on the applied voltage as calculated by solving self-consistently the transport equations, namely the electron continuity equations, the Poisson equation, and the current transport equation. Shown are the conduction band edge (full line) and the valence band edge (dotted line) over the distance from the indium tin oxide (ITO) electrode. The poly(ethylene dioxythiophene)-layer (PEDOT) is up to 50 nm and assumed as a *p*-type semiconductor. The bulk heterojunction is between 50 and 110 nm distance from the ITO electrode and assumed as one ambipolar semiconductor. The metal contact is more than 110 nm away from the ITO electrode. The potential within the bulk of the solar cell is nearly flat for voltages near V_{oc} (a) and shows a constant potential decrease, which can be seen clearly for 0 V (b) without band bending.

distance R_p on the illumination intensity is taken into account by adding a photoconductive part to the dark shunt $R_{p,dark}$ as described elsewhere.³ This is done by adding a second photoconductive parallel resistor $R_{photosh}$, where the photoconductivity is proportional to the light intensity P_{light} .

Figure 3 shows typical current–voltage characteristics of

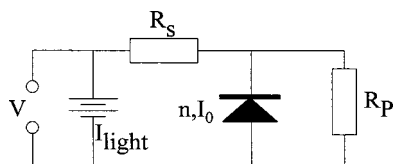


FIG. 2. Equivalent circuit diagram of the macroscopic model for describing a solar cell with one diode. The total current for a given voltage V is the sum of the single currents through the diode, which is represented by the parameters n and I_0 , the shunt resistance R_p , the limiting series resistance R_s , and the light current I_{light} .

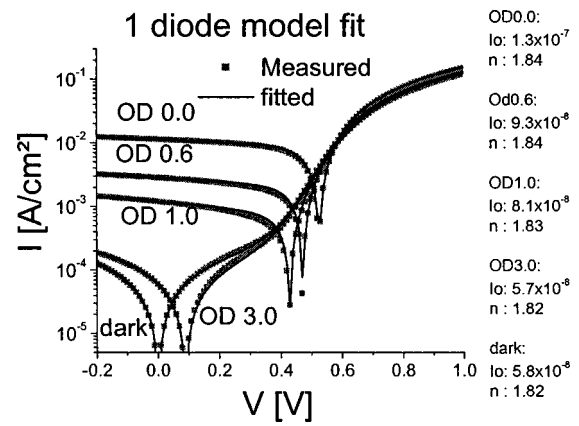


FIG. 3. I – V curves measured under various light intensities (boxes) with fitted curves using standard one-diode model (line). Values for the parameters n and I_0 are given for each light intensity. The light intensity is given by the value of optical density of the various gray filters and the light intensity of 110 mW/cm² @ OD0.

bulk heterojunction solar cells measured under different illumination intensities together with the optimal fit as gained from Eq. (1). The fit parameters are collected in Table I where R_p is calculated with $R_{p,dark}$ and $R_{photosh}$ via the light intensity. Experimental data have been taken on devices using a poly(3-hexyl thiophene) (P3HT) as donor and a [6,6]-phenyl C₆₁-butyric acid methyl ester (the fullerene PCBM) as the acceptor. Details on the device production are given elsewhere.⁴

The general quality of the fits is satisfying. The shunt (characteristic in the voltage regime between -0.2 and 0.2 V) and the diode turn on (characteristic in the voltage regime between 0.3 and 0.6 V) of the dark I – V curve is correctly reproduced with a meaningful set of parameters. Please note, that the slope of the I/V characteristic in the diode turn on regime is dominantly influenced by the ideality factor n . Also the illuminated I – V curves can be correctly reproduced, however, in order to properly describe the open circuit voltage under increasing illumination density, a continuous increase of the saturation current I_0 is necessary. The variation of I_0 by a factor of 2 is significant and gives an equivalent shift of the open circuit voltage by nearly 50 mV. However, the variation of dark diode parameters under illumination cannot be justified, since it would correspond to a change of the dark diode itself under illumination. This is in conflict with Eq. (1), where I_{light} is the only parameter sensitive to

TABLE I. Fit parameters n , I_0 , and R_s for I – V curves measured under various light intensities, fitted using standard one-diode model. The light intensity is given by the value of optical density (OD), the various gray filters and the light intensity of 110 mW/cm² @ OD0. R_p is calculated with the dark shunt $R_{p,dark} = 1540 \Omega \text{ cm}^2$ parallel to a photoconductive resistor with the photoconductivity $1/R_{photosh} = 5.3 \times 10^{-5} (\Omega \text{ cm}^2 \text{ mW})^{-1}$.

OD filter	n	Saturation current I_0 (A/cm ²)	R_s ($\Omega \text{ cm}^2$)
0.0	1.84	1.3×10^{-7}	2.2
0.6	1.84	9.3×10^{-8}	2.5
1.0	1.81	8.1×10^{-8}	2.5
3.0	1.82	5.7×10^{-8}	2.6
Dark	1.82	5.7×10^{-8}	2.4

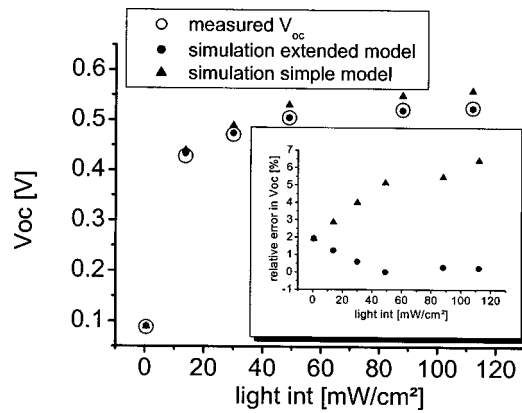


FIG. 4. The open circuit voltage (V_{oc}) over the light intensity as measured (open circles \circ), fitted with the standard one-diode model (closed triangle \blacktriangle), and fitted with the extended model (closed circle \bullet). The inset shows the relative error of the V_{oc} value of the standard model and the extended model to the measured value.

illumination. A fixed set of parameters I_0 and n does not correctly reproduce the illumination dependency of V_{oc} (see Fig. 4): the higher the light intensity the larger the error in V_{oc} . Also a two diode model, where the second diode is implemented as a Shockley–Read–Hall-recombination diode^{7,8} could not explain the illumination intensity of the V_{oc} , independent on the ideality factors of these two diodes.

The discrepancy discussed earlier brings up the deficiencies of the one diode model given in Eq. (1). In order to remove this discrepancy, we suggest a more sophisticated model. It was shown previously³ that the photoinduced current of bulk heterojunction solar cells is strongly driven by the internal electrical field. This is not further surprising for devices with active layers in the 100 nm regime, and a constant electrical field (as seen in Fig. 1) further supports these findings. Applying now an external bias close to the built-in voltage V_{bi} will minimize this field. Consequently, a reduction of the electrical field is expected to reduce the average mean carrier distance, given in Eq. (2):

$$\text{mean distance} = \tau \times \mu \times \frac{(V - V_{bi})}{L}, \quad (2)$$

where τ is the average lifetime of the carriers, μ is the carrier mobility, and L the thickness of the sample. Equation (2) suggests that I_{light} should not be regarded as constant with voltage. If the average mean carrier distance is smaller than the thickness of the sample, just the fraction (mean distance)/(layer thickness) will reach the contacts and can be extracted from the solar cell. Therefore in the expansion of the one diode model, the dependence of I_{light} on the voltage will be taken into account. Similar models have been used to describe I – V curves of amorphous silicon (a -Si)-solar cells,^{9,10} when transport is limited by the field driven average mean-carrier distance.

First, the photogenerated charge carrier flux density is calculated. Since the solar cells discussed in this article show no or only negligible carrier losses (an internal quantum efficiency of $\sim 100\%$ and an external quantum efficiency of $\sim 80\%$ was measured),⁴ the carrier flux density can be esti-

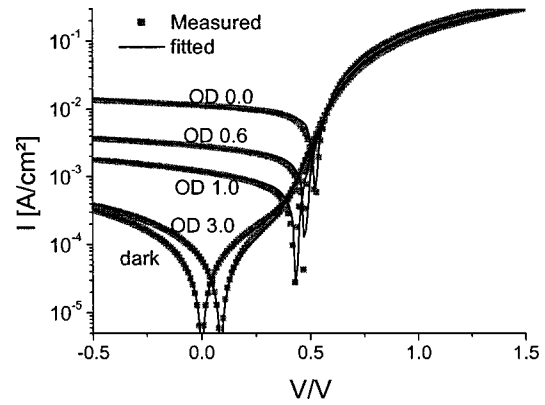


FIG. 5. I – V curves measured under various light intensities (boxes) with fitted curves using the one-diode Model with nonconstant light current I_{light} (line). Values for the model parameters are given in Table II and are the same for each light intensity. The light intensity is given by the value of optical density of the various gray filters and the light intensity of 110 mW/cm² @ OD0.

mated directly from the short circuit current I_{sc} , which is equivalent to I_{light} (0 V). The photogenerated charge carriers are now driven by the potential difference between the internal built-in voltage V_{bi} ^{5,11} and the applied voltage V . The number of carriers which can be extracted from the device equals the total number of carriers multiplied by the ratio of the mean distance to the thickness of the sample, where this ratio should be in the range from 0...1. The overall photogenerated current I_{light} can be rewritten as

$$I_{light}(V) = \begin{cases} -|I_{sc}| & \text{if } \mu \times \tau \times (-V + V_{bi})/L > L \\ |I_{sc}| & \text{if } \mu \times \tau \times (V - V_{bi})/L > L \\ |I_{sc}| \times \mu \times \tau \times (-V + V_{bi})/L^2 & \text{else} \end{cases} \quad (3)$$

Reversal of the photocurrent between the fourth and the first quadrant is a consequence of a field driven light generated current. In forward direction the photocurrent contributes to the total current, e.g., due to photoconductivity. Equation (3) does not contain direct carrier recombination. Please note that in the case of recombination losses, I_{sc} in Eq. (3) has to be replaced by I_{sc0} , the maximum possible (optical limited) primary photocurrent which can be extracted under large reverse bias. Alternatively, more sophisticated models can be taken into account. Such models, regarding the influence of direct recombination processes have been discussed for a -Si devices.^{9,10} We applied these models to fit the bulk heterojunction data presented in Figs. 3 and 5 and it turned out, that direct recombination processes are not relevant for the presented bulk heterojunction data. However, we cannot exclude that these more sophisticated models^{9,10} are relevant for other bulk heterojunction materials or material combinations.

This extended one diode model composed of the standard one diode model Eq. (1) and the field depended light current Eq. (3) will now be tested on the experimental data set already shown in Fig. 3. The fitting of I – V curves is done by iteratively minimizing the mean least error χ^2 , which is given by the sum over the differences between the measured and fitted currents at each voltage [Eq. (4)]:

TABLE II. Fit parameters n , I_0 , R_s , $R_{p\text{-dark}}$, $1/R_{\text{photoshunt}}$, μ , τ , and V_{bi} for I - V curves measured under various light intensities, fitted using expanded one-diode Model with nonconstant I_{light} .

Parameter	Value
n	1.79
I_0 (A/cm ²)	4.8×10^{-8}
R_s (Ω cm ²)	2.1
$R_{p\text{-dark}}$ (Ω cm ²)	1540
$1/R_{\text{photoshunt}}$ (Ω cm ² mW) ⁻¹	5.3×10^{-5}
μ (cm ² /V s)	0.001
τ (s)	7.1×10^{-6}
V_{bi} (V)	0.61

$$\chi^2 = \sum_V [I_{\text{measured}}(V) - I_{\text{fitted}}(V)]^2 + \{\log[I_{\text{measured}}(V)] - \log[I_{\text{fitted}}(V)]\}^2. \quad (4)$$

With this iterative method dark diode parameters I_0 , n , R_s , and $R_{p\text{-dark}}$ are determined first. Second, keeping the dark diode parameters constant, the mobility μ and the carrier life time τ are determined by fitting the illuminated I - V curves. The set of parameters are listed in Table II for the light-current Eq. (3). The mobility is kept constant at 10^{-3} cm²/V s in accordance to literature values for P3HT¹² and PCBM¹³. Figure 5 shows again the experimental data compared to the fitted data as calculated from Table II. Again, excellent agreement is observed, but, different to the simple one diode model, the expanded model can reach this high quality of the fit with one and the same set of parameters. Most important, the open circuit voltage is fitted correctly over more than three orders in illumination with one set of parameters (Fig. 4).

Plotting the I - V curve on a linear scale reveals a small deviation in the fourth quadrant just before the open circuit voltage is observed (Fig. 6). This deviation is supposed to originate from the rather crude assumption in the model that all photogenerated carriers have identical mobility and lifetime. Due to the neglect of a distribution of mobility and lifetime values, the photocurrent is slightly overestimated at the opening of the diode and therefore the fill factor is also slightly overestimated.

As a benefit of the expanded model, a mean carrier life time τ is estimated, which is elaborate to obtain otherwise. The value for τ of several microseconds determined by fitting experimental data with the expanded diode model is similar to the carrier lifetimes determined from transient absorption measurements on polymer bulk heterojunction films.¹⁴ The value of the fitted built-in voltage of 0.61 V is also in good agreement with the measured open circuit voltage.

CONCLUSION

A modified one diode model is suggested to describe the illumination dependence of current-voltage characteristics

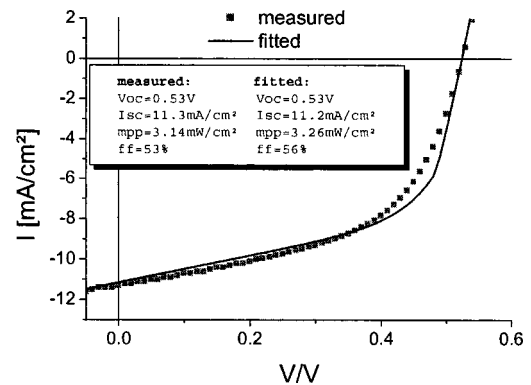


FIG. 6. The fourth quadrant of measured (boxes) and fitted (line) I - V curve in a linear scale for 110 mW/cm². The values for the short circuit current (I_{sc}), open circuit voltage (V_{oc}), maximum power point, and (FF) are given for both fitted and measured I - V curves.

of polymeric bulk heterojunction solar cells. This modified one-diode model takes into account the field dependence of the photogenerated current. Excellent results are obtained for the expanded model. I - V curves of bulk heterojunction solar cells are properly described with one set of parameters, especially the dependence of the open circuit voltage on the light intensity is reproduced very precisely. Moreover, the model allows an estimation of the built-in voltage V_{bi} and of the mean carrier lifetime τ or of the $\mu\tau$ product if the mobility μ of the tested material is unknown. Small deviations in the fourth quadrant are explained that the model does not take the statistical distribution of the mobility and lifetime into account. All in all the model provides insight into the working mechanisms of bulk heterojunction solar cells and will help to identify the critical parameters for further improvements of these cells.

¹J. Nelson, *Curr. Opin. Solid State Mater. Sci.* **6**, 87 (2002).

²T. Martens *et al.*, *Mater. Res. Soc. Symp. Proc.* **725**, 169 (2002).

³C. Waldauf, P. Schilinsky, J. Hauch, and C. J. Brabec, *Thin Solid Films* (in press).

⁴P. Schilinsky, C. Waldauf, and C. Brabec, *Appl. Phys. Lett.* **81**, 3885 (2002).

⁵C. Brabec, A. Cravino, D. Meissner, N. S. Sariciftci, M. T. Rispens, and L. Sanchez, *Thin Solid Films* **403-404**, 368 (2002).

⁶S. M. Sze, *Semiconductor Devices* (Wiley, New York, 1985).

⁷W. Shockley and W. T. Read, *Phys. Rev.* **87**, 835 (1952).

⁸R. N. Hall, *Phys. Rev.* **87**, 387 (1952).

⁹R. S. Crandall, *J. Appl. Phys.* **54**, 7176 (1983).

¹⁰J. Merten, J. M. Asensi, C. Voz, A. V. Shah, R. Platz, and J. Andreu, *IEEE Trans. Electron Devices* **45**, 423 (1998).

¹¹C. J. Brabec, A. Cravino, D. Meissner, N. S. Sariciftci, T. Fromherz, M. T. Rispens, L. Sanchez, and J. C. Hummelen, *Adv. Funct. Mater.* **11**, 374 (2001).

¹²H. Siringhaus *et al.*, *Nature (London)* **401**, 685 (1999).

¹³V. D. Mihailescu *et al.*, *Adv. Funct. Mater.* **13**, 43ff (2003).

¹⁴I. Montanari, A. F. Nogueira, J. Nelson, J. R. Durrant, C. Winder, M. A. Loi, N. S. Sariciftci, and C. Brabec, *Appl. Phys. Lett.* **81**, 3001 (2002).